Analysis of nanoparticle delivery to tumours

Stefan Wilhelm, Anthony J. Tavares, Qin Dai, Seiichi Ohta, Julie Audet, Harold F. Dvorak and Warren C. W. Chan

Abstract | Targeting nanoparticles to malignant tissues for improved diagnosis and therapy is a popular concept. However, after surveying the literature from the past 10 years, only 0.7% (median) of the administered nanoparticle dose is found to be delivered to a solid tumour. This has negative consequences on the translation of nanotechnology for human use with respect to manufacturing, cost, toxicity, and imaging and therapeutic efficacy. In this article, we conduct a multivariate analysis on the compiled data to reveal the contributions of nanoparticle physicochemical parameters, tumour models and cancer types on the low delivery efficiency. We explore the potential causes of the poor delivery efficiency from the perspectives of tumour biology (intercellular versus transcellular transport, enhanced permeability and retention effect, and physicochemical-dependent nanoparticle transport through the tumour stroma) as well as competing organs (mononuclear phagocytic and renal systems) and present a 30-year research strategy to overcome this fundamental limitation. Solving the nanoparticle delivery problem will accelerate the clinical translation of nanomedicine.

The possibility of engineering nanoparticles that selectively detect and destroy cancer cells in the body remains an exciting concept[1–3]. This has led researchers to engineer a myriad of different nanoparticle designs exhibiting unique physicochemical properties (for example, size, shape and surface chemistry) and programmed with a multitude of biological and medical functions[4,5]. Examples include polymer-based nanostructures that can be assembled to target cancer[6] or inorganic nanoparticles that can produce heat upon light irradiation to photothermally eradicate tumours[7]. Nanoparticles can be further equipped to carry one or more contrast agents[8–10], release drugs via a trigger, such as pH[11–13] or enzymatic catalysis[14,15], or to have a combination of diagnostic and therapeutic agents (that is, theranostics)[16,17]. Molecular-based assembly techniques can also be used to build nanosystems with multiple functions such as targeting tumours and enabling clearance from the body[18]. Many studies have shown the utility of nanoparticles for detecting and killing cancer cells *in vitro* (for example, in cell cultures) and *in vivo* (for example, in mouse models); however, the clinical translation of nanoparticles has been limited.

In this article, we explore the influence of delivery on the efficacy of nanoparticles for cancer-targeting applications. Delivery is important because systemically administered nanoparticle carriers cannot function as designed if they do not access the diseased cells and tissues at a sufficiently high dosage[19–21]. Nanoparticles, once injected into the body, face both physical and biological barriers (for example, diffusion, flow and shear forces, aggregation, protein adsorption, phagocytic sequestration and renal clearance) that affect the percentage of administered nanoparticles reaching target diseased tissue and cells[22–25]. We provide a quantification of the delivery efficiency of nanoparticles, review the fundamental principles and the current state and misconception of the biological mechanisms of the nanoparticle delivery process, and describes research strategies that may enhance the delivery efficiency.

Delivery efficiency and consequences

How many nanoparticles accumulate in a tumour? Upon systemic administration, the mononuclear phagocytic system (MPS) and the renal clearance pathway compete with the tumour for nanoparticles. The MPS is a network of organs (most notably the liver and spleen) that contains phagocytic cells that take up nanoparticles, while the renal (kidney) system excretes nanoparticles smaller than 5.5 nm in hydrodynamic diameter[26–29]. Nanoparticles that escape the aforementioned biological barriers have the opportunity to interact with the tumour tissue. The percentage of administered nanoparticles that can achieve this is defined as the nanoparticle delivery efficiency[30].

To determine the current delivery efficiency to solid tumours, we used SciFinder and Google Scholar databases and the search term 'nanoparticle delivery', and identified 224 manuscripts (FIG. 1a,b). We started by analysing the most recent publications and did not observe any significant variance in the median of the delivery efficiency over the past 10 years. Thus, we conclude that these data represent the current stage of development. From this compilation of studies, the data from 117 reports were tabulated (Supplementary information S1 (table)) and standardized to calculate the delivery efficiency based on a non-compartmental linear trapezoidal analysis model[31]. This method is commonly used in pharmacokinetic studies to determine area-under-the-curve (AUC) values, and it enabled the quantification of the AUC for a given nanoparticle–tumour interaction, providing temporal and spatial information with a minimum of three time points (FIG. 1c). The remaining 107 papers were excluded from our analysis because of insufficient time points (FIG. 1b; Supplementary information S2 (table)). More time points might have allowed a more precise calculation of the AUC, but very few researchers presented data with more than three time points (FIG. 1b). In many cases, authors were contacted to provide additional information to accurately calculate the AUC. Our analysis revealed that a median of 0.7% of the injected dose (ID) of the nanoparticles reached the tumour (this value was derived from 232

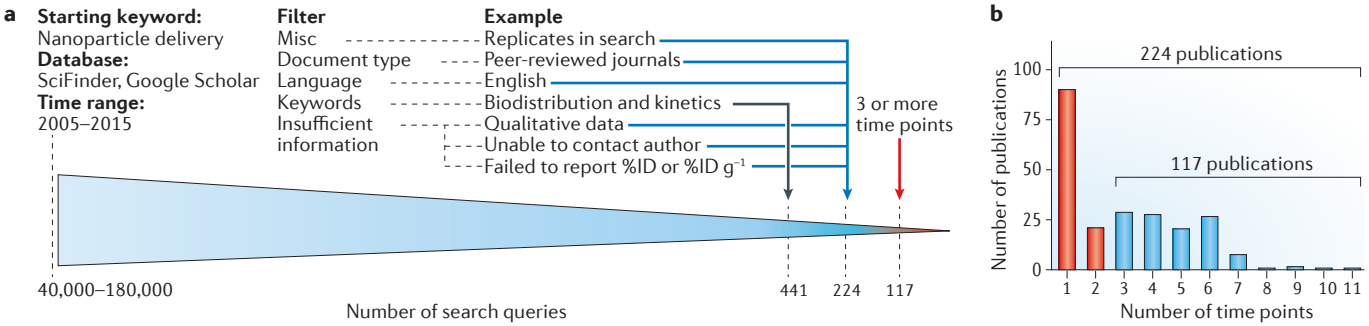

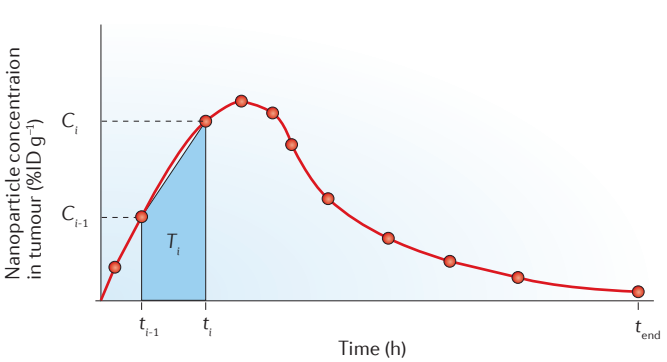

$$\text{Trapezoid } (T_i) = 0.5\,(C_i + C_{i-1})\,(t_i - t_{i-1}) \quad (1)$$

$$\text{AUC}_{\text{Tumour}} = \sum_{i=1}^{n} T_i \quad (2)$$

$$\text{Delivery efficiency} = \frac{\text{AUC}_{\text{Tumour}}}{t_{\text{end}}}\,(m_{\text{Tumour}}) \quad (3)$$

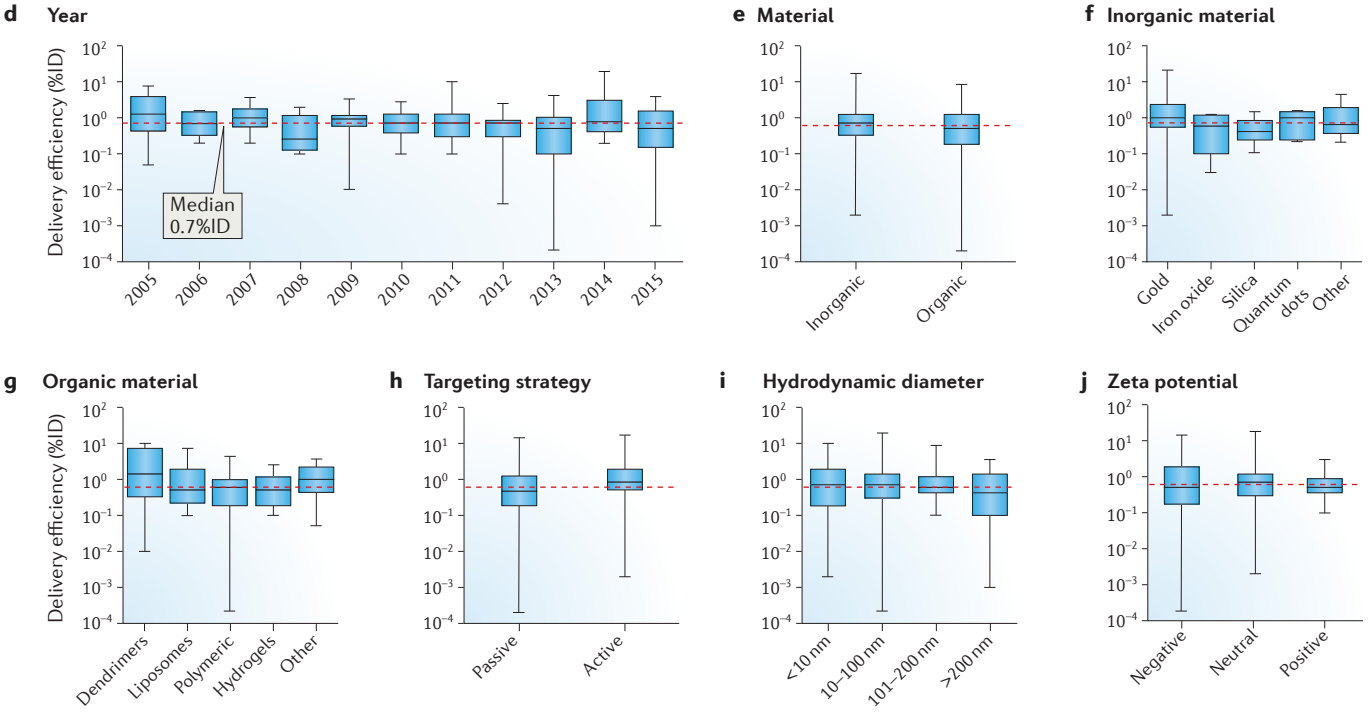

data sets) and that the median delivery efficiency has not improved in the past 10 years (FIG. 1d). This suggests that only 7 out of 1,000 administered nanoparticles actually entered a solid tumour in a mouse model. We used the median rather than the arithmetic mean to describe the delivery efficiency because the variability of data sets was high and the median is less affected by extreme values. We also provide alternative ways to interpret the delivery efficiency (for example, %ID per gram of tissue) in the Supplementary information.

Several trends may be observed in the data. First, nanoparticles composed of inorganic materials tend to provide a higher delivery efficiency than those made from organic materials (0.8% and 0.6%ID, respectively). Second, particles with hydrodynamic diameters smaller than 100 nm tend to show a higher delivery efficiency than larger particles (0.7% and 0.6%ID, respectively). Third, the delivery efficiency of nanoparticles exhibiting neutral zeta potentials, as defined from −10 to +10 mV, tends to be higher than the delivery efficiency of nanoparticles with positive (>10 mV) or negative (<−10 mV) zeta potentials (0.7%, 0.6% and 0.5%ID, respectively). Fourth, active-targeting strategies tend to outperform passive-targeting strategies, affording delivery efficiencies of 0.9% and 0.6%ID, respectively. Fifth, rod-shaped nanoparticles tend to exhibit a higher delivery efficiency compared with spherical, plate or flake, and other shapes, with values of 1.1%, 0.7%, 0.6% and 0.9%ID, respectively. Last, orthotopic tumour models tend to display higher delivery efficiencies than heterotopic tumour models (FIG. 1e–m; TABLE 1).

In 4 out of the 117 publications, delivery efficiencies higher than 5%ID were reported; the only physicochemical commonalities of these studies were the use of nanoparticles with hydrodynamic diameters less than 100 nm and near-neutral zeta potentials (Supplementary information S1 (table)). However, it is difficult to draw more specific conclusions from the analysis of these four papers[32–35].

A multivariate analysis was further conducted to determine the contribution of a single parameter or combination of biological, physical and chemical parameters to the 0.7%ID. This analysis was undertaken to tease apart the effect of multiple interacting factors on the delivery efficiency. The data showed that the cancer type and the tumour model were major factors; however, they influenced the delivery efficiency of organic and inorganic nanoparticles in different manners as shown in TABLE 2 and Supplementary information S3–S5 (multivariate analysis) (a lower *P* value suggests a higher probability for the contribution of a specific parameter on the delivery efficiency).

Consequences of low nanoparticle delivery efficiency. We used a simple dosimetry analysis to estimate the consequences of using nanoparticles with 0.7%ID delivery efficiency for treating patients with cancer. Although an accurate determination of the human dose on the basis of animal studies is inherently complex, our analysis provides a simple, quantitative and general approximation that can be refined in future analyses.

We are evaluating two drug-loading strategies for nanoparticles: drug encapsulation in the nanoparticle core and drug loading on the nanoparticle surface. Provided that the efficiency of drug loading is the same for both strategies, the amount of drug is proportional to the cube and square of the nanoparticle radius, for each respective strategy (FIG. 2; Supplementary information S6,S7 (table, estimation)). For our estimation, we used a nanoparticle (60 nm in diameter) carrying anticancer drugs with a molecular weight of 500 g mol^{-1}, a half maximal inhibitory concentration (IC_{50}) value of 1.0 μM and a delivery efficiency of 1.0%ID as an example. To achieve the IC_{50} in a tumour (volume of 0.5 cm^3) of a mouse (body weight of 20 g), it would be necessary to inject 1.2×10^{12} nanoparticles or a dose of 6.5 mg kg^{-1} provided that the nanoparticles encapsulated 20 wt% of the drug, which is a typical nanoparticle drug-loading capacity. If drugs were loaded on the particle surface with a density of one drug molecule per nanometer squared, the required dose would increase to 2.8×10^{12} nanoparticles or 15.7 mg kg^{-1}. Such doses should be feasible in mice, because a typical injection dose for a mouse study is approximately 10 mg kg^{-1}. However, if the dose is scaled from a mouse to a human, it becomes more difficult to achieve the required quantity; that is, one would need 2.7×10^{14} drug-encapsulated nanoparticles (19 mg m^{-2}) or 6.4×10^{14} surface-loaded nanoparticles (45 mg m^{-2}) for one person using a body-surface-area-based dosing strategy[36]. This would result in a systemic administration of 90 ml (drug encapsulation strategy) or 213 ml (drug surface loading strategy) of colloidal nanoparticle dispersions (assuming a nanoparticle concentration of 5.0 nM) into the patient to elicit a therapeutic effect similar to that in a mouse model (Supplementary information S7 (estimation)). Calculations for other nanoparticle sizes are presented in Supplementary information S8 (figure).

Our rough estimations using a delivery efficiency of 1.0%ID suggest that there are serious problems for the translation of cancer targeting nanoparticles for human use. First, the required amount of nanoparticles that need to be injected into humans would be high and would require the ability to scale up nanoparticle production, which is not a trivial task. Colloidally stable nanoparticles are commonly synthesized on a small scale for use in academic settings and for small animal (for example, mouse) models. This scale of synthesis is easily achieved for most nanoparticle types. When synthesis is scaled to prepare a large amount of nanoparticles in one batch, the nanoparticle quality and function may be compromised (for example, through the formation of aggregates, a polydisperse size distribution or shape irregularities). Second, the cost of nanoparticles for conventional use in patients may be prohibitively high because of the large number of nanoparticles required per injection dose. Third, the relatively high injection volume provides a technical limitation for using nanoparticles in patients; further concentration of nanoparticles to reduce the dispersion volume can compromise their colloidal stability and cause irreversible aggregation and/or shorten the shelf life. Fourth, because approximately 99%ID of all administered nanoparticles

◀ Figure 1 | **Analysis of nanoparticle delivery efficiency to solid tumours from studies published in 2005–2015. a** | Procedure used for the literature survey. **b** | Diagram showing the distribution of time points for the 224 publications that were identified by our survey. **c** | The linear trapezoidal method was used to calculate the area-under-the-curve (AUC_{Tumour}) of the plot of nanoparticle concentration in the tumour tissue as a function of time. Equations (1–3) were used to calculate the delivery efficiency, in which T_i is the area of the trapezoid obtained by multiplying the time interval t_{i-1} to t_i by the corresponding concentration interval C_{i-1} to C_i (according to equation (1)). The AUC_{Tumour} is calculated by summation of all trapezoids (T_i) from $i = 1$ to $i = n$; [AUC_{Tumour}] = %ID h g^{-1} (equation (2)). Finally, the delivery efficiency (in %ID units) is obtained by dividing the AUC_{Tumour} by the time of the end-point (t_{end}) of the study and multiplying by the average tumour mass for each study (m_{Tumour}; equation (3)). **d**–**m** | Box-and-whisker plots of the delivery efficiency data. The boxes represent the 25th to 75th percentiles and the black solid lines indicate the median values. The red dashed lines denote the median of the nanoparticle delivery efficiency derived from all 232 data sets (that is, 0.7%ID).

will interact with off-target tissues, high nanoparticle doses increase the risk of toxicity. Last, for engineering nanoparticles for cancer cell and subcellular targeting, the dosage requirement and cost may be even higher. It is possible that the amount of nanoparticles reaching cancer cells and their subcellular compartments *in vivo* is much less than 0.7%ID because nanoparticles need to cross the tumour extracellular matrix to reach the cancer cells. These nanoparticles may interact nonspecifically with non-malignant cells and other structural tissue components. A central strategy for addressing all of these issues is by increasing the delivery efficiency. For example, if delivery efficiencies improve from 1% to 10%ID, the injection volume for nanoparticles that follow a drug encapsulation strategy would decrease from 90 to 9 ml.

Table 1 | **Delivery efficiency and the number of data sets used from Figure 1d–m**

Category	Delivery efficiency [%ID]*	Number of data sets
All data sets	0.7	232
Year		
2005	1.4	8
2006	0.7	8
2007	1.0	24
2008	0.3	8
2009	0.9	11
2010	0.8	14
2011	0.7	27
2012	0.7	14
2013	0.5	35
2014	0.8	38
2015	0.5	45
Material		
Inorganic	0.8	86
Organic	0.6	137
Inorganic material		
Gold	1.0	45
Iron oxide	0.6	8
Silica	0.4	13
Quantum dots	0.9	5
Other	0.6	14
Organic material		
Dendrimers	1.4	7
Liposomes	0.5	27
Polymeric	0.6	62
Hydrogels	0.5	18
Other	0.9	23
Targeting strategy		
Passive	0.6	175
Active	0.9	57

Tumour-targeting mechanisms

Elucidating the specific mechanisms involved in nanoparticle–tumour interactions will help to develop more effective strategies to increase the delivery efficiency beyond 0.7%ID. The delivery of nanoparticles to tumours is based on specific and nonspecific cellular interactions. Specific (or active) targeting relies on functionalizing the surface of nanoparticles with ligands that are complementary to the target sites, which may be peritumoural and intratumoural blood vessels, the extracellular matrix, tumour cells or intracellular targets. In nonspecific (or passive) targeting, the nanoparticle surface is coated only with anti-fouling and/or stabilizing agents. The current view is that nanoparticles cross the tumour vascular barrier through intercellular gaps and are retained in the tumour owing to pressure created by poor lymphatic drainage — a process termed 'enhanced permeability and retention' (EPR)[37]. Nanoparticles could be further retained in the tumour by active targeting[32,38]. In this article, we focus on intratumoural nanoparticle targeting.

Nanoparticle extravasation

Once nanoparticles reside in tumour blood vessels, they can extravasate into the tumour microenvironment. This section describes where and how nanoparticles extravasate from the tumour vasculature, and compares and contrasts the intercellular versus transendothelial transport mechanisms.

Tumour blood vessels. A basic understanding of tumour blood vessels is important to explain nanoparticle–tumour interactions and transportation. When nanoparticles are injected into tumour-bearing animals, they rapidly pass from the systemic circulation to chaotic vessels that supply the tumour with oxygen and nutrients. The tumour vasculature is highly abnormal, exhibiting an uneven distribution with zones of both increased and sparse vascular density, hierarchical disorganization, serpentine structure and irregular branching, and includes vascular malformations that form arteriovenous shunts[39,40]. Tumour vascular density is generally highest at the tumour/host interface; by contrast, central portions of tumours tend to be less well vascularized and often exhibit zones of necrosis owing to insufficient blood supply[41,42]. There are at least six distinctly different types of tumour blood vessels: feeding arteries, mother vessels, glomeruloid microvascular proliferations (GMP), vascular malformations, capillaries and draining veins[39,43–51] (FIG. 3a).

Nanoparticles are likely to cross the vascular barrier and enter the tumour compartment through mother vessels. These vessels are derived from normal venules and capillaries and are the first angiogenic type of blood vessel to form. They exhibit abnormal hyperpermeability to plasma proteins because they are lined by a single, thin layer of flattened endothelial cells, have disrupted basement membranes and have little or no pericyte coverage[47–49,52,53]. These vessels also leak both

Table 1 (cont.) | **Delivery efficiency and the number of data sets used from Figure 1d–m**

Category	Delivery efficiency [%ID]*	Number of data sets
Hydrodynamic diameter		
<10 nm	0.7	14
10–100 nm	0.7	115
100–200 nm	0.6	54
>200 nm	0.4	34
Zeta potential		
Negative	0.5	65
Neutral	0.7	118
Positive	0.6	14
Shape		
Spherical	0.7	188
Rod	0.8	23
Plate or flake	0.6	12
Other	0.7	9
Tumour model		
Allograft heterotopic	0.7	90
Allograft orthotopic	1.0	13
Xenograft heterotopic	0.6	90
Xenograft orthotopic	1.1	38
Cancer type		
Brain	0.8	28
Breast	0.6	63
Cervix	0.6	20
Colon	0.6	24
Liver	0.7	15
Lung	0.1	10
Ovary	0.5	8
Pancreas	0.8	10
Prostate	0.6	8
Skin	1.3	35

Zeta potentials were reported at pH 7.4. Negative, neutral and positive zeta potentials are defined as <−10 mV, −10 to 10 mV and >10 mV, respectively. *Median.

plasma and plasma proteins, which leads to increased local haematocrit and blood viscosity, and thus sluggish blood flow. As a consequence, nanoparticles inside tumour vessels tend to move slowly or become stagnant. This provides enough time for the nanoparticles to diffuse out of the vessel and into the extracellular matrix of the tumour.

Intercellular extravasation. The predominant belief in the nanotechnology community is that nanoparticles extravasate from the tumour blood vessels into the tumour microenvironment through gaps between adjacent endothelial cells. This is one of the key fundamental principles for the EPR effect[37,54–56]. Normal vessels are lined by an endothelial cell monolayer that is held together by specific junctions of two types — adherens and tight junctions — and only allow small molecules, such as oxygen, glucose, salts, water and metabolic waste products, to pass through the space between normal capillary endothelial cells[57]. By contrast, the endothelial cells of tumour blood vessels have irregular sizes and shapes, and have ruffles and projections that may extend across vessel lumens because of rapid vessel growth, chaotic flows and the uneven distribution of oxygen and nutrients. As a result, adjacent endothelial cells adhere to each other less tightly, forming interendothelial cell gaps across the vessel wall. These gaps (100–500 nm in size, depending on the tumour type and stage, as derived from mouse models[58]) are typically located in mother vessels and, to a lesser extent, in other vessels, such as GMP[46,48,49,53]. The EPR effect suggests that nanoparticles transport passively through these gaps. Normal capillaries also have intercellular gaps, which tend to be smaller than those in the mother vessels. Small proteins (for example, horseradish peroxidase) have been reported to cross normal capillaries — both through caveolae (transcellular) and normal capillary junctions[59] (FIG. 3b) — but larger macromolecules cannot. Thus, most nanoparticles with a diameter of more than 10 nm will be too large to extravasate from normal capillaries.

Transcellular extravasation. An alternative hypothesis is that nanoparticles can extravasate into tumours via a transendothelial cell pathway. Normal venule and capillary endothelial cells contain a structure termed vesiculo–vacuolar organelles (VVOs), which span the cytoplasm from the lumen to the ablumen (FIG. 3b). VVOs are composed of an extensive plexus of interconnected cytoplasmic vesicles and vacuoles, the membranes of which collectively constitute a surface area several times that of the venular plasma membrane[59]. They provide a pathway for the extravasation of plasma during acute vascular hyperpermeability induced by vascular endothelial growth factors (VEGFs) and other vascular permeabilizing agents[60]. VVOs contribute to mother vessel formation by providing the necessary membrane to the cell surface, which allows a four- to fivefold vessel enlargement. As a result, mother vessels contain fewer VVO vesicles than the normal venular endothelium from which they originate. Despite the reduced number of vesicles available for transendothelial transport, the distance VVOs have to traverse across thinned mother vessel endothelium is also reduced[41] (FIG. 3b). Both horseradish peroxidase and ferritin have been shown to cross solid tumour blood vessels via the VVO pathway[59,60].

Which extravasation mechanism is more important? It is unclear which pathways dominate the extravasation of macromolecules and nanoparticles in tumours. Macromolecules can extravasate from mother vessels and GMP by way of intercellular gaps; however, these gaps are exceedingly rare, as was determined in mother vessels induced by an adenoviral vector expressing murine VEGFA[164]. In addition, some or many of the reported

interendothelial cell gaps may actually represent open transcellular VVOs. VVOs are located close to and interact with lateral endothelial cell junctions and could thus give the appearance of interendothelial gaps. It was shown using serial section electron microscopy that many of these openings are in fact transendothelial cell pores[57]. Distinguishing between intercellular gaps and transendothelial cell pores is difficult, and intercellular gaps can only be demonstrated definitively by labelling the margins with selective junctional markers such as vascular endothelial cadherin; to our knowledge, this has never been attempted. However, the mechanisms and pathways that mediate nanoparticle transport to the tumour are important. If the extravasation is mediated primarily by the transcellular route, nanoparticles that will actively target this transport pathway can be designed. At present, the nanotechnology community has not investigated this transport mechanism. Instead, a heavy emphasis has been placed on studying nanoparticle transport through intercellular gaps via the EPR mechanism — an approach that has thus far yielded poor delivery efficiency. Therefore, there is a need to probe the tumour endothelium transport mechanism to guide the future design of nanoparticles.

Table 2 | ***P* values for effects on delivery efficiency***

Effect parameter	*P* value
All materials	
Cancer type	<0.0001
Targeting strategy	0.0082
Material	0.0210
Hydrodynamic diameter	0.0633
Shape	0.0992
Tumour model	0.2748
Zeta potential	0.3782
Material and tumour model	<0.0001
Cancer type and hydrodynamic diameter	<0.0001
Material and targeting strategy	0.0178
Hydrodynamic diameter and hydrodynamic diameter	0.0478
Organic Material	
Cancer type	<0.0001
Tumour model	0.0001
Organic material	0.0088
Hydrodynamic diameter	0.0185
Shape	0.0479
Zeta potential	0.1493
Targeting strategy	0.7350
Cancer type and hydrodynamic diameter	<0.0001
Tumour model and hydrodynamic diameter	<0.0001
Zeta potential and zeta potential	0.0068
Hydrodynamic diameter and hydrodynamic diameter	0.0078
Inorganic material	
Inorganic material	<0.0001
Targeting strategy	0.0040
Hydrodynamic diameter	0.0086
Cancer type	0.0180
Zeta potential	0.1491
Shape	0.9013

**P* values for main effects, quadratic effects and two-factor interaction effects on delivery efficiency were obtained using analysis of variance (ANOVA) in combination with a multiple regression model for 'all materials', 'organic materials' and 'inorganic materials'. A Box-Cox transformation was performed on the delivery efficiency and the parameter 'hydrodynamic diameter' was log-transformed. Multiple factor interactions could not be solved for 'inorganic materials' owing to limitations of the data sets. A detailed description and interpretation of the multivariate analysis is described in the Supplementary information S3–S5 (multivariate analysis).

Intratumoural nanoparticle interactions

Once the nanoparticles have crossed the vascular barrier, they have to navigate through the tumour microenvironment to reach and target cells or specific intratumoural structures. This section provides a description of these tumour biological barriers and explains the current view of how the physicochemical properties of nanoparticles dictate the transport process in the tumour microenvironment.

Components of the tumour microenvironment. Nanoparticles interact with heterogeneous components of the tumour stroma (that is, non-malignant cells such as fibroblasts, pericytes and immune cells) and parenchyma (that is, malignant cells) after extravasation from the tumour vasculature. In solid tumours, the structural rigidity is supported by extracellular matrix components such as collagen, fibronectin, hyaluronan, fibrin and proteoglycans synthesized by fibroblasts[61]. Tumours are highly heterogeneous because the composition of parenchyma and stroma cells, and the type and ratio of the support and secreted proteins vary depending on tumour type and stage[62,63]. The interstitial fluid pressure inside the tumour can be elevated by a factor of 10–40 compared with normal tissues[64,65], creating pressure gradients and heterogeneous flow in the interstitium. This pressure can influence the transport and distribution of chemotherapeutics, imaging agents, macromolecules and nanoparticles in the tumour[24]. Furthermore, the high tumour interstitial fluid pressure increases the outward interstitial flow to the stroma and lymphatics with increased fluid transport to the nearest 'sentinel' lymph node; coupled with lymphangiogenesis, which is found in some but by no means all solid tumours, these characteristics strongly correlate with tissue invasiveness and metastasis[65].

Intratumoural targeting. After extravasation, the physicochemical-dependent transport and penetration depth of nanoparticles in the tumour matrix are likely to be influenced by the tumour type, size and stage because of

the specific tumour microenvironment properties (as described in the previous section)[66,67]. The general consensus is that smaller nanoparticles penetrate more deeply into the tumour extracellular matrix away from the blood vessel, whereas their larger counterparts are restricted to the immediate vicinity of the vascular extravasation point[66,68,69]. The physicochemical properties may determine whether nanoparticles coated with tumour-cell-targeting aptamers, antibodies, peptides and/or small molecules are able to interact with malignant cells.
A head-to-head comparison of active and passive targeting reveals a lack of significant difference in tumour accumulation[32,70,71].
To fully elucidate the nanoparticle fate in the tumour tissue, we have to move beyond 2D images[72] and employ 3D imaging and quantify nanoparticle–cell interactions *in vivo* to describe, confirm and evaluate specific intratumoural nanoparticle targeting.

Organs competing with tumours

The MPS and renal system compete with the tumour for circulating nanoparticles[26–28] (FIG. 4) and sequester and/or eliminate 99% of the administered nanoparticles. To increase the delivery efficiency, it is necessary to decrease the blood clearance by these two biological systems and/or to increase the accumulation of nanoparticles in the tumour during the first or second pass (that is, early-on in circulation).

Mononuclear phagocytic system.
Nanoparticles are identified by the MPS as foreign substances that need to be sequestered, degraded and eliminated. The MPS consists mainly of the liver, spleen, lymph nodes, bone marrow, skin and other organs containing resident phagocytic cells such as macrophages. Resident macrophages in the MPS organs are derived from circulating monocytes and can be phenotypically diverse and heterogeneous in an organ[73]. Most administered nanoparticles are sequestered by the liver and the spleen, and thus the discussion will focus on these two organs.

Macrophages in the liver include Kupffer cells and motile macrophages, and reside in liver sinusoids along with fenestrated endothelial cells (FIG. 4a). While nanoparticles flow through the liver sinusoidal capillaries, it has been suggested that scavenger receptors on Kupffer cells recognize the opsonins adsorbed on the nanoparticle surface and engulf them. The way in which the cells process the nanoparticles varies based on the nanoparticle type and chemistry; for example, large inorganic nanoparticles can reside in these cells for long periods of time, whereas organic nanoparticles are more rapidly degraded and eliminated[74].

The specificity and role of spleen macrophages in terms of nanoparticle uptake has not been fully investigated. The spleen is compartmentalized into the red and white pulp that are separated by a marginal zone, and sinuses with pores of approximately 3 μm in diameter[75]. The red pulp contains macrophages that are involved in erythrocyte degradation[73], whereas the marginal zone macrophages, B cells and dendritic cells provide defence against pathogens. Metallophilic macrophages and tingible body macrophages reside in the white pulp and are responsible for innate immunity and clearing of apoptotic cells, respectively[76]. Macrophages in either the red or white pulp can potentially take up circulating nanoparticles, but the specifics remain unclear.

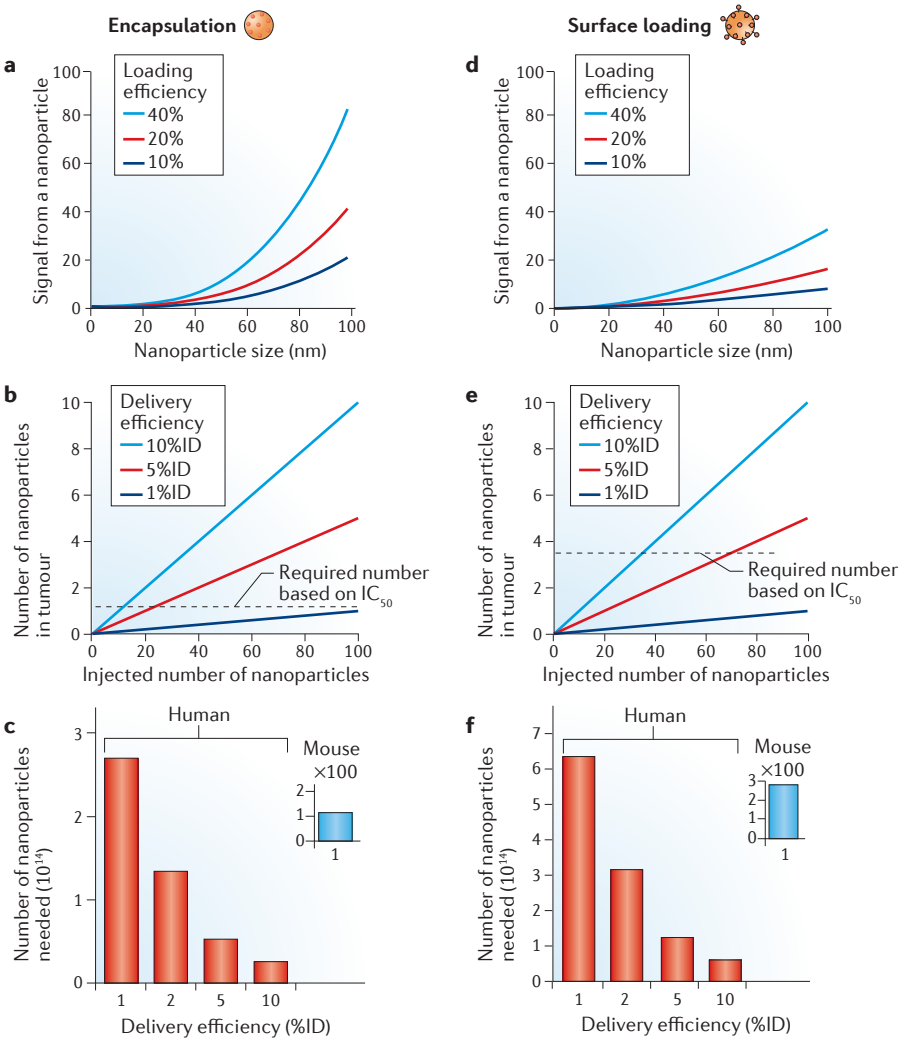

Figure 2 | **Estimation of nanoparticle dose for human tumour treatment.** Drug or imaging agent encapsulation strategies are shown in panels **a**–**c**. Surface loading strategies are shown in panels **d**–**f**. Drugs or imaging agents can be loaded either inside (panel **a**) or on the surface (panel **d**) of nanoparticles. The therapeutic efficacy or imaging signal from a nanoparticle is proportional to the cube of the particle radius in the former case and the square in the latter case. The amount of systemically administered nanoparticles that reach the tumour can be calculated as a function of the delivery efficiency (panels **b** and **e**). By setting required therapeutic efficacy or imaging signal levels for the tumour, such as the half maximal inhibitory concentration (IC_{50}), the required dose of nanoparticles to treat the tumour of a particular size can be estimated. Using the assumptions mentioned in Supplementary information S6,S7 (table, estimation), the dose of nanoparticles needed for the treatment of a tumour in mice can be calculated (panels **c** and **f**). This dose can be converted into a human equivalent dose by using a body-surface-area relationship[36].

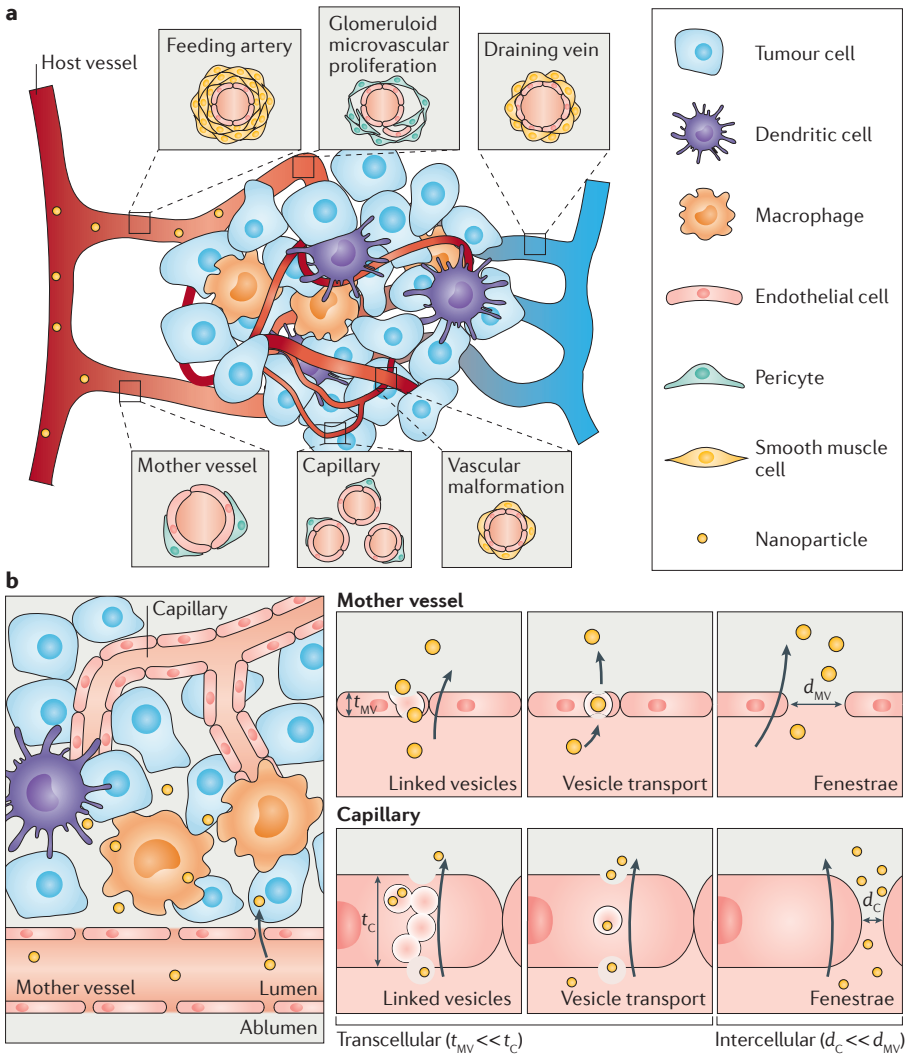

Figure 3 | **Tumour blood vessels and mode for nanoparticle extravasation in mother vessels versus capillaries. a** | Mother vessels arise from pre-existing normal venules and capillaries. They are characterized by thinned or compressed endothelial cells, degraded basement membranes and pericyte detachment. As a result of these structural changes, mother vessels are highly permeable not only to small molecules but also to large plasma proteins. Mother vessels are unstable and, over time, differentiate into glomeruloid microvascular proliferations, vascular malformations and capillaries. Glomeruloid microvascular proliferations are tortuous vessels that are composed of irregular layers of pericytes and endothelial cells with multiple, very small vascular lumens. Vascular malformations are similar in size to mother vessels but have reacquired a smooth muscle coating. Capillaries form from mother vessels and from glomeruloid microvascular proliferations. Feeding arteries and draining veins arise from arterio-venogenesis and are enlarged, tortuous blood vessels that supply and drain angiogenic vasculature, respectively. **b** | In the transcellular pathway, nanoparticles enter luminal endothelial cell vesicles, which are transported across the endothelial cell, allowing discharge of cargo into the extravascular space. This can occur through a series of linked vesicles or through a single vesicle in thinned mother vessel endothelium. Mother vessels may also include fenestrae and open pores through which macromolecules can extravasate. In the interendothelial cell extravasation mechanism, nanoparticles are transported through gaps of 100–500 nm in diameter. d_C, the intercellular gap distance in capillaries; d_{MV}, the intercellular gap distance in mother vessels; t_C, the thickness of endothelial cells lining the capillaries; t_{MV}, the thickness of endothelial cells lining the mother vessels.

Macrophage uptake mechanisms. The predominant mechanism of nanoparticle sequestration by macrophages is phagocytosis, although nanoparticles can also be taken up by macropinocytosis, clathrin-mediated and caveolin-mediated endocytosis, and by other endocytic pathways[77]. It is well known that low-density lipoproteins and bacteria are taken up through scavenger receptors, and this mechanism has been adapted to explain how nanoparticles are sequestered. In some studies, nanoparticles were shown to be taken up through scavenger receptors[78,79]; however, more receptors may be involved, because engineered nanoparticles are more chemically diverse than pathogens and low-density lipoproteins. Thus, the mechanism of nanoparticle interaction with MPS organs and macrophages is likely to be more complex.

When nanoparticles are administered into the body, their physicochemical properties change. The nanoparticles interact with serum proteins to form a 'protein corona' and may aggregate. The corona is diverse and consists of ions, opsonins and other serum proteins[80,81]. This process has been described as a change in the molecular identity of the nanoparticle, from a 'synthetic identity' that describes the measured size, shape and surface chemistry post-synthesis to a 'biological identity' that describes the physicochemical properties after interaction with the biological fluid[82]. It is the biological identity that determines the interaction with the cells. Analysis of the protein corona of over 70 formulations of gold nanoparticles revealed unique serum protein coatings for each formulation, and thus it is unclear how a single protein or a combination of these proteins mediate their interactions with macrophages[83,84].

Researchers have observed interesting trends in nanoparticle–macrophage interactions. Larger nanoparticles are cleared more rapidly than smaller nanoparticles, and particles with cationic surfaces show the strongest macrophage uptake, followed by those with anionic surface charge and then by those with zero net surface charge. For example, poly(ethylene glycol) (PEG)-coated gold nanoparticles that are 90 nm in diameter have a 4-fold higher uptake by J774A.1 macrophages than their 15- and 30-nm counterparts with similar surface charge[83]. Comparable trends were observed *in vivo* for gold nanoparticles between 10 and 250 nm: the 10-nm gold nanoparticles showed an increased distribution throughout the body, whereas the 250-nm gold nanoparticles were retained to a greater extent in MPS organs[85]. To escape macrophage uptake and extend the circulation lifetime of nanoparticles *in vivo*, researchers typically coat the nanoparticles with neutral polymers, such as PEG or erythrocyte membranes, to camouflage the particles from these cells. A longer circulation lifetime increases the chance for nanoparticles to accumulate in the tumour. There is a direct correlation between the length and density of PEG ligands and the blood half-life of nanoparticles[66]. However,

these 'stealth' nanoparticle formulations have not fully solved the sequestration and targeting problem. Thus, it is important to obtain a detailed understanding of how the MPS organs and specific macrophage cells interact with nanoparticles.

Renal clearance. The kidney glomeruli have three layers: a fenestrated endothelium, a glomerular basement membrane and a lining epithelium[86] (FIG. 4b). The charge- and size-selective permeation are the functions of the latter two layers, respectively[87]. The basement membrane is a structural gel composed of a heterogeneous network of type IV collagen, fibronectin and heparan sulfate proteoglycan, among other components, and has a net polyanionic charge[86]. The epithelium lining contains filtration slits of 4–6 nm in width[87] and allows the passage of nanoparticles smaller than this size cut-off. Nanoparticles filtered out of the blood in glomeruli pass into the proximal convoluted tubule and are eventually eliminated in urine. Nanoparticles filtered from glomeruli can also be endocytosed by cells that line the proximal tubules before they reach the bladder[88].

Perspective

The single key word that will continue to stimulate nanomedicine research in the next 30 years is 'translation'. Nanoparticles are designed to alter the biodistribution and pharmacokinetics of a small molecule drug or contrast agent in patients and enable the delivery of a larger dose to the targeted diseased tissue in an effort to improve the therapeutic index, reduce systemic toxicity and/or offer better imaging signals. These advantages have been dampened by the lack of translation to patient care, despite the large investment (more than US$1 billion in North America in the past 10 years) and success in imaging and treating tumours in mouse models. As a result, nanomedicine has acquired a reputation of being 'hype' that cannot deliver and has not transformed patient cancer care as it promised 15 years ago.

Nanoparticles can be approved for human use by health agencies if they offer an improvement in diagnosis, therapeutic index and/or a reduction of toxicity. At present, only a few non-targeted nanoparticle formulations (for example, Abraxane and Doxil) have been clinically approved[30,89–91] because they alter the toxicological profile of drugs in patients. Interestingly, these formulations did not yield significant improvements in therapeutic index or diagnostics[21,92,93]. The approval process was based on end-outcome measurements, which are strongly related to how the nanoparticles alter the transportation and function of the small molecule anticancer agent in the body. This suggests the importance of understanding and controlling the delivery of nanoparticles *in vivo*.

Researchers are starting to develop non-conventional strategies to improve the delivery efficiency, including: normalization of tumour vasculature[94–98]; use of bacteria and cells to deliver nanoparticles to tumours[99–106]; engineering nanoparticles that can dynamically change size or create different entry pathways into tumours to increase penetration depth[18,107–110]; manipulation of the MPS system[111–113]; and surface coatings comprising cell-membrane components derived from leukocytes or proteins, such as CD47, that bind and inhibit phagocyte ingestion[114–116]. However, the clinical relevance of these studies cannot be determined because they are still early in development.

We need to consider a more rational and longer-term strategic approach to overcome the nanoparticle delivery problem. The community must take a step back and evaluate the principles that have guided the field and assess whether targeting is possible. Many researchers regard a delivery efficiency of 0.7%ID to represent nonspecific interaction rather than specific targeting. The current underlying principles of nanoparticle targeting have not produced the desired clinical outcomes, and if these principles remain unquestioned, the next 30 years will only provide more unsatisfactory results. If nanoparticles cannot accumulate in solid tumours and reach target tumour cells, how can they effectively work as designed?

We suggest a 30-year systematic and coordinated strategy to enable the community to make decisions that move the field forward (FIG. 5). The key question that needs to be addressed is: can nanoparticles target diseased tissues? This can only be answered by conducting careful and systematic studies. The next 10 years should focus on probing the fundamental interactions of nanoparticles with organs and tissues that accumulate, sequester or eliminate nanoparticles (such as the liver, spleen and kidney), as well as the interactions between nanoparticles and tumours, with respect to the physicochemical

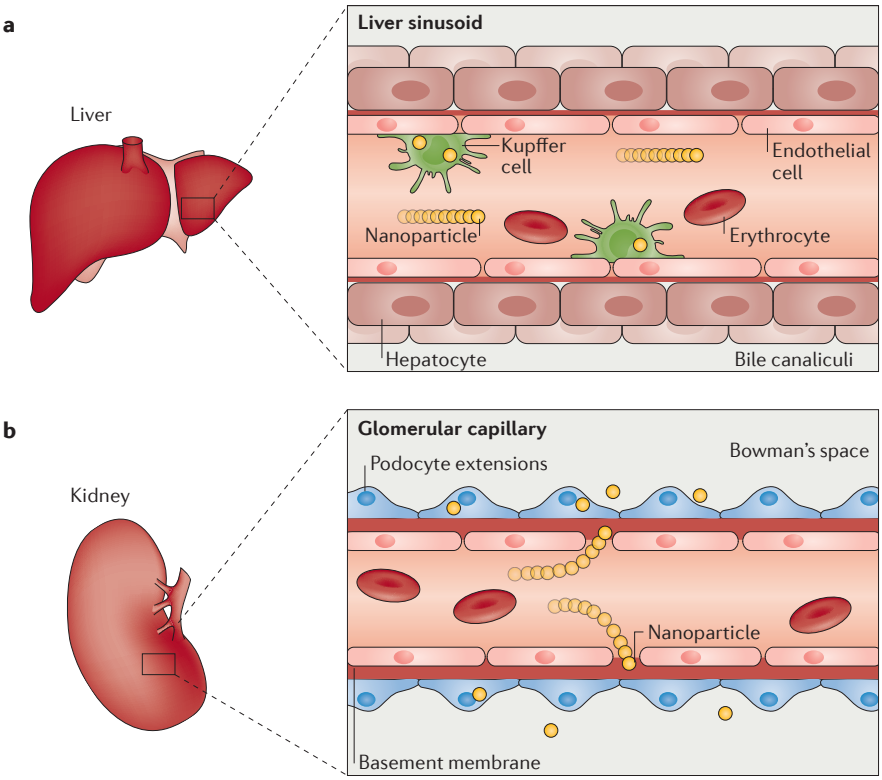

Figure 4 | **Mechanisms for nanoparticle elimination from the bloodstream. a** | The liver is the primary organ of the mononuclear phagocytic system that entraps a vast majority of the administered nanoparticle dose. Phagocytic cells, such as Kupffer cells, line the liver sinusoid. **b** | If the hydrodynamic diameter of a nanoparticle is smaller than 5.5 nm, it may be filtered from the blood via the kidneys and excreted in urine. Other major organs that are involved in the removal of nanoparticles from the blood-stream include the spleen, lymph nodes and the skin.

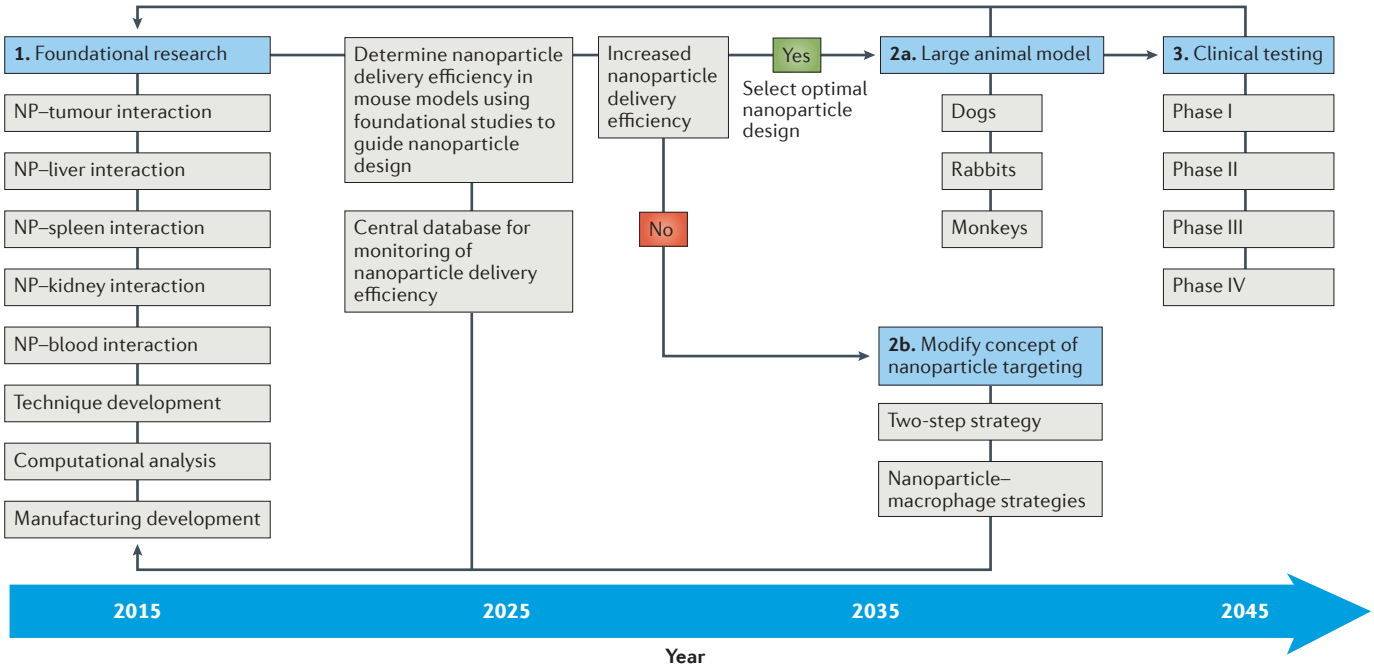

Figure 5 | **Proposed 30-year strategy for nanoparticle delivery research.** Current research in using nanoparticles *in vivo* has focused on innovative design and demonstration of utility of these nanosystems for imaging and treating cancer. The poor clinical translation has encouraged the researchers in the field to investigate the effect of nanoparticle design (for example, size, shape and surface chemistry) on its function and behaviour in the body in the past 10 years. From a cancer-targeting perspective, we do not believe that nanoparticles will be successfully translated to human use if the current 'research paradigm' of nanoparticle targeting continues because the delivery efficiency is too low. We propose a long-term strategy to increase the delivery efficiency and enable nanoparticles to be translated to patient care in a cost-effective manner from the research stage. A foundation for the field will be built by obtaining a detailed view of nanoparticle–organ interaction during nanoparticle transport to the tumour, using computational strategies to organize and simulate the results and the development of new tools to assess nanoparticle delivery. In addition, we propose that these results should be collected in a central database to allow progress in the field to be monitored and correlations to be established. A 30-year strategy was proposed and seemed to be a reasonable time frame because the first liposome system was reported in 1965 (REF. 122) and the first liposome formulation (Doxil) was approved by the US Food and Drug Administration (FDA) in 1995 (REFS 91,92). This 30-year time frame may be shortened as a research foundation has already been established but only if the community can parse the immense amount of currently published data. NP, nanoparticle.

properties of the nanoparticles. These studies must challenge the current paradigm of why the MPS sequesters nanoparticles, whether the nanoparticles are taken into tumours solely by the EPR effect, whether nanoparticles can be transported effectively into and through tumours, and whether the pressure inside tumours can be measured and altered to improve nanoparticle transport. These are merely starting points, and there are many other questions that need to be answered. These studies should drill down to the details, from the synthetic and biological identities of the nanoparticles to the biological systems from host, organ, tissue, cell and molecular perspectives. There is a need to develop techniques and tools that allow quantitative analysis of these fundamental questions. These studies need to be multi-parametric (multiple particle types with multiple cell and tissue systems) and may require computational tools to deconvolve the data and present models of interactions. Computational tools and mathematical modelling can be used to analyse tumour interactions and response to drugs and nanoparticles in both preclinical and clinical stages[117–119]. Finally, a database should be designed to track and organize the data to enable the determination of relationships between biological systems and the physicochemical properties of nanoparticles. We have started to build an internet-based repository that allows researchers to input new data, which will generate an open access database of nanoparticle tumour delivery efficiency that can be analysed in real-time.

The second 10 years could focus on using these fundamental studies to design optimal nanoparticle systems for targeting tumours and to test these formulations in various animal models. By analysing diverse animal models in the same study, the delivery efficiency can be determined and the mechanisms involved can be identified. Achieving the desired research goals will require multidisciplinary teams with a detailed plan of action. Again, the focus should be on measuring the delivery efficiency and therapeutic indexes using designs that were optimized in the first 10 years. If the delivery efficiency cannot be increased, the community will need to change their way of thinking about nanomedicine. Because we know that nanoparticles are heavily sequestered by macrophages, perhaps a better scenario may be to combine nanoparticles with macrophages for use in immunotherapy or to assess two- or multistage strategies (for example, first removing macrophages followed by the injection of therapeutic nanoparticles)[120].

The final 10-year period will need to focus on clinical trials and making use of the optimal nanoparticle formulations. The results need to be fed back to the foundational studies and database so that the data can be mined to assess the fundamental interactions of nanoparticles with biological systems from the mouse model to the human level. An example of an early cross-animal analysis was recently conducted for the assessment of CALAA-01, a nanoparticle formulation for small intefering RNA delivery[121]. Despite the fact that our proposed 30-year approach

is slower and more controlled than might be hoped for in advancing nanomedicine, it has the potential to generate a foundation that will serve the field and facilitate nanomedicine translation in the latter part of this century. Furthermore, this approach will allow researchers and clinicians to truly assess the potential of nanotechnology for cancer applications and enable the community to make rational research decisions.

We must admit that our current approach is broken, and that is why we have not observed significant clinical translation of cancer nanomedicines. Many academic studies focused on the potential of nanoparticles for *in vivo* medical applications and showed that nanoparticles may be delivered into tumours by the EPR effect. However, publishing 'proof-of-concept' studies will only lead to curing mice and will unlikely translate to patient care, irrespective of the number of nanoparticle design permutations used for cancer-targeting studies. Despite the lack of translational progress, nanotechnology remains an exciting topic of research and does have promise for improving patient care. The main advantages of using nanoparticles are that they can be engineered with precise functional properties and can access biological systems and compartments. However, our inability to control the nanoparticle transport inside the body presents a major limitation for using nanotechnology to diagnose and treat cancer, as well as diabetes, cardiovascular disorders and other diseases for which nanotechnology is actively researched.

Stefan Wilhelm, Anthony J. Tavares, Qin Dai, Seiichi Ohta, Julie Audet and Warren C. W. Chan are at the Institute of Biomaterials and Biomedical Engineering, University of Toronto, 164 College St, Toronto, Ontario M5S 3G9, Canada.

Julie Audet and Warren C. W. Chan are at the Donnelly Center for Cellular and Biomolecular Research, University of Toronto, 160 College St, Toronto, Ontario M5S 3E1, Canada.

Warren C. W. Chan is at the Departments of Chemistry, Materials Science and Engineering, and Chemical Engineering, University of Toronto, 164 College St, Toronto, Ontario M5S 3G9, Canada.

Seiichi Ohta is at the Center for Disease Biology and Integrative Medicine, The University of Tokyo, 7-3-1 Hongo, Bunkyo-ku, Tokyo 113–0033, Japan.

Harold F. Dvorak is at the Center for Vascular Biology Research, Department of Pathology, Beth Israel Deaconess Medical Center and Harvard Medical School, 330 Brookline Ave, Boston, Massachusetts 02215, USA.

Correspondence to W.C.W.C.
warren.chan@utoronto.ca

Article number: 16014
doi:10.1038/natrevmats.2016.14
Published online 26 Apr 2016

1. Peer, D. *et al.* Nanocarriers as an emerging platform for cancer therapy. *Nat. Nanotechnol.* **2**, 751–760 (2007).
2. Rao, W. *et al.* Chitosan-decorated doxorubicin-encapsulated nanoparticle targets and eliminates tumor reinitiating cancer stem-like cells. *ACS Nano* **9**, 5725–5740 (2015).
3. Min, Y., Caster, J. M., Eblan, M. J. & Wang, A. Z. Clinical translation of nanomedicine. *Chem. Rev.* **115**,11147–11190 (2015).
4. Nel, A. E. *et al.* Understanding biophysicochemical interactions at the nano–bio interface. *Nat. Mater.* **8**, 543–557 (2009).
5. Albanese, A., Tang, P. S. & Chan, W. C. W. The effect of nanoparticle size, shape, and surface chemistry on biological systems. *Annu. Rev. Biomed. Eng.* **14**, 1–16 (2012).
6. Endres, T. *et al.* Optimising the self-assembly of siRNA loaded PEG–PCL–IPEI nano-carriers employing different preparation techniques. *J. Control. Release* **160**, 583–591 (2012).
7. Huang, X., El-Sayed, I. H., Qian, W. & El-Sayed, M. A. Cancer cell imaging and photothermal therapy in the near-infrared region by using gold nanorods. *J. Am. Chem. Soc.* **128**, 2115–2120 (2006).
8. Wolfbeis, O. S. An overview of nanoparticles commonly used in fluorescent bioimaging. *Chem. Soc. Rev.* **44**, 4743–4768 (2015).
9. Attia, M. F. *et al.* Biodistribution of X-ray iodinated contrast agent in nano-emulsions is controlled by the chemical nature of the oily core. *ACS Nano* **8**, 10537–10550 (2014).
10. Kircher, M. F. *et al.* A brain tumor molecular imaging strategy using a new triple-modality MRI-photoacoustic-Raman nanoparticle. *Nat. Med.* **18**, 829–834 (2012).
11. Guo, X. Shi, C., Wang, J., Di, S. & Zhou, S. pH-triggered intracellular release from actively targeting polymer micelles. *Biomaterials* **34**, 4544–4554 (2013).
12. Gao, W., Chan, J. M. & Farokhzad, O. C. pH-responsive nanoparticles for drug delivery. *Mol. Pharmaceut.* **7**, 1913–1920 (2010).
13. Cheng, R., Meng, F., Deng, C., Klok, H.-A. & Zhong, Z. Dual and multi-stimuli responsive polymeric nanoparticles for programmed site-specific drug delivery. *Biomaterials* **34**, 3647–3657 (2013).
14. Hu, Q., Katti, P. S. & Gu, Z. Enzyme-responsive nanomaterials for controlled drug delivery. *Nanoscale* **6**, 12273–12286 (2014).
15. de la Rica, R., Aili, D. & Stevens, M. M. Enzyme-responsive nanoparticles for drug release and diagnostics. *Adv. Drug Deliv. Rev.* **64**, 967–978 (2012).
16. Chen, F., Ehlerding, E. B. & Cai, W. Theranostic nanoparticles. *J. Nucl. Med.* **55**, 1919–1922 (2014).
17. Chen, Q. *et al.* Drug-induced self-assembly of modified albumins as nano-theranostics for tumor-targeted combination therapy. *ACS Nano* **9**, 5223–5233 (2015).
18. Chou, L. Y. T., Zagorovsky, K. & Chan, W. C. W. DNA assembly of nanoparticle superstructures for controlled biological delivery and elimination. *Nat. Nanotechnol.* **9**, 148–155 (2014).
19. Bae, Y. H. & Park, K. Targeted drug delivery to tumors: myths, reality and possibility. *J. Control. Release* **153**, 198–205 (2011).
20. Wang, A. Z., Langer, R. & Farokhzad, O. C. Nanoparticle delivery of cancer drugs. *Annu. Rev. Med.* **63**, 185–198 (2012).
21. Park, K. Facing the truth about nanotechnology in drug delivery. *ACS Nano* **7**, 7442–7447 (2013).
22. Lazarovits, J., Chen, Y. Y., Sykes, E. A. & Chan, W. C. W. Nanoparticle–blood interactions: the implications on solid tumour targeting. *Chem. Commun.* **51**, 2756–2767 (2015).
23. Nichols, J. W. & Bae, Y. H. Odyssey of a cancer nanoparticle: from injection site to site of action. *Nano Today* **7**, 606–618 (2012).
24. Jain, R. K. & Stylianopoulos, T. Delivering nanomedicine to solid tumors. *Nat. Rev. Clin. Oncol.* **7**, 653–664 (2010).
25. Florence, A. T. "Targeting" nanoparticles: the constraints of physical laws and physical barriers. *J. Control. Release* **164**, 115–124 (2012).
26. Choi, H. S. *et al.* Renal clearance of quantum dots. *Nat. Biotechnol.* **25**, 1165–1170 (2007).
27. Liu, J. *et al.* PEGylation and zwitterionization: pros and cons in the renal clearance and tumor targeting of near-IR-emitting gold nanoparticles. *Angew. Chem. Int. Ed. Engl.* **52**, 12572–12576 (2013).
28. Liu, J. *et al.* Passive tumor targeting of renal-clearable luminescent gold nanoparticles: long tumor retention and fast normal tissue clearance. *J. Am. Chem. Soc.* **135**, 4978–4981 (2013).
29. Yu, M. & Zheng, J. Clearance pathways and tumor targeting of imaging nanoparticles. *ACS Nano* **9**, 6655–6674 (2015).
30. Dawidczyk, C. M. *et al.* State-of-the-art in design rules for drug delivery platforms: lessons learned from FDA-approved nanomedicines. *J. Control. Release* **187**, 133–144 (2014).
31. Chiou, W. L. Critical evaluation of the potential error in pharmacokinetic studies of using the linear trapezoidal rule method for the calculation of the area under the plasma level-time curve. *J. Pharmacokinet. Biopharm.* **6**, 539–546 (1978).
32. Sykes, E. A., Chen, J., Zheng, G. & Chan, W. C. W. Investigating the impact of nanoparticle size on active and passive tumor targeting efficiency. *ACS Nano* **8**, 5696–5706 (2014).
33. Tsai, C.-C. *et al.* Biodistribution and pharmacokinetics of ^{188}Re-liposomes and their comparative therapeutic efficacy with 5-fluorouracil in C26 colonic peritoneal carcinomatosis mice. *Int. J. Nanomed.* **6**, 2607–2619 (2011).
34. Kukowska-Latallo, J. F. *et al.* Nanoparticle targeting of anticancer drug improves therapeutic response in animal model of human epithelial cancer. *Cancer Res.* **65**, 5317–5324 (2005).
35. Sadekar, S., Ray, A., Janàt-Amsbury, M., Peterson, C. M. & Ghandehari, H. Comparative biodistribution of PAMAM dendrimers and HPMA copolymers in ovarian-tumor-bearing mice. *Biomacromolecules* **12**, 88–96 (2011).
36. Reagan-Shaw, S., Nihal, M. & Ahmad, N. Dose translation from animal to human studies revisited. *FASEB J.* **22**, 659–661 (2008).
37. Maeda, H., Nakamura, H. & Fang, J. The EPR effect for macromolecular drug delivery to solid tumors: improvement of tumor uptake, lowering of systemic toxicity, and distinct tumor imaging *in vivo*. *Adv. Drug Deliv. Rev.* **65**, 71–79 (2013).
38. Ruoslahti, E., Bhatia, S. N. & Sailor, M. J. Targeting of drugs and nanoparticles to tumors. *J. Cell Biol.* **188**, 759–768 (2010).
39. Dvorak, H. F., Nagy, J. A., Dvorak, J. T. & Dvorak, A. M. Identification and characterization of the blood vessels of solid tumors that are leaky to circulating macromolecules. *Am. J. Pathol.* **133**, 95–109 (1988).
40. Warren, B. A. in *Tumor Blood Circulation: Angiogenesis, Vascular Morphology and Blood Flow of Experimental and Human Tumors* (ed. Peterson, H.-I.) 1–47 (CRC Press, 1979).
41. Nagy, J. A. *et al.* Permeability properties of tumor surrogate blood vessels induced by VEGF-A. *Lab. Invest.* **86**, 767–780 (2006).
42. Dvorak, H. F. Rous-Whipple Award Lecture. How tumors make bad blood vessels and stroma. *Am. J. Pathol.* **162**, 1747–1757 (2003).
43. Dvorak, H. F. in *The Endothelium: A Comprehensive Reference* (ed. Aird, W.) 1457–1470 (Cambridge Univ. Press, 2007).
44. Zeng, H. *et al.* Orphan nuclear receptor TR3/Nur77 regulates VEGF-A-induced angiogenesis through its transcriptional activity. *J. Exp. Med.* **203**, 719–729 (2006).
45. Paku, S. & Paweletz, N. First steps of tumor-related angiogenesis. *Lab. Invest.* **65**, 334–346 (1991).
46. Nagy, J. A., Benjamin, L., Zeng, H., Dvorak, A. M. & Dvorak, H. F. Vascular permeability, vascular hyperpermeability and angiogenesis. *Angiogenesis* **11**, 109–119 (2008).
47. Chang, S. H. *et al.* VEGF-A induces angiogenesis by perturbing the cathepsin–cysteine protease inhibitor balance in venules, causing basement membrane degradation and mother vessel formation. *Cancer Res.* **69**, 4537–4544 (2009).
48. Nagy, J. A., Chang, S. H., Shih, S. C., Dvorak, A. M. & Dvorak, H. F. Heterogeneity of the tumor vasculature. *Semin. Thromb. Hemostasis* **36**, 321–331 (2010).
49. Pettersson, A. *et al.* Heterogeneity of the angiogenic response induced in different normal adult tissues by vascular permeability factor/vascular endothelial growth factor. *Lab. Invest.* **80**, 99–115 (2000).
50. Fidler, I. J., Yano, S., Zhang, R. D., Fujimaki, T. & Bucana, C. D. The seed and soil hypothesis: vascularisation and brain metastases. *Lancet Oncol.* **3**, 53–57 (2002).
51. Sundberg, C. *et al.* Glomeruloid microvascular proliferation follows adenoviral vascular permeability factor/vascular endothelial growth factor-164 gene delivery. *Am. J. Pathol.* **158**, 1145–1160 (2001).
52. Nagy, J. A., Shih, S. C., Wong, W. H., Dvorak, A. M. & Dvorak, H. F. Chapter 3. The adenoviral vector angiogenesis/lymphangiogenesis assay. *Methods Enzymol.* **444**, 43–64 (2008).
53. Nagy, J. A., Dvorak, A. M. & Dvorak, H. F. Vascular hyperpermeability, angiogenesis, and stroma generation. *Cold Spring Harbor Perspect. Med.* **2**, a006544 (2012).

54. Kobayashi, H., Watanabe, R. & Choyke, P. L. Improving conventional enhanced permeability and retention (EPR) effects; what is the appropriate target? *Theranostics* **4**, 81–89 (2013).
55. Prabhakar, U. *et al.* Challenges and key considerations of the enhanced permeability and retention effect for nanomedicine drug delivery in oncology. *Cancer Res.* **73**, 2412–2417 (2013).
56. Matsumura, Y. & Maeda, H. A. New concept for macromolecular therapeutics in cancer chemotherapy: mechanism of tumoritropic accumulation of proteins and the antitumor agent smancs. *Cancer Res.* **46**, 6387–6392 (1986).
57. Dvorak, H. F. Tumors: wounds that do not heal–redux. *Cancer Immunol. Res.* **3**, 1–11 (2015).
58. Hobbs, S. *et al.* Regulation of transport pathways in tumor vessels: role of tumor type and microenvironment. *Proc. Natl Acad. Sci. USA* **95**, 4607–4612 (1998).
59. Dvorak, A. M. *et al.* The vesiculo-vacuolar organelle (VVO): a distinct endothelial cell structure that provides a transcellular pathway for macromolecular extravasation. *J. Leukocyte Biol.* **59**, 100–115 (1996).
60. Feng, D., Nagy, J. A., Hipp, J., Dvorak, H. F. & Dvorak, A. M. Vesiculo-vacuolar organelles and the regulation of venule permeability to macromolecules by vascular permeability factor, histamine, and serotonin. *J. Exp. Med.* **183**, 1981–1986 (1996).
61. Pickup, M. W., Mouw, J. K. & Weaver, V. M. The extracellular matrix modulates the hallmarks of cancer. *EMBO Rep.* **15**, 1243–1253 (2014).
62. Box, C., Rogers, S. J., Mendiola, M. & Eccles, S. A. Tumour-microenvironmental interactions: paths to progression and targets for treatment. *Semin. Cancer Biol.* **20**, 128–138 (2010).
63. Eccles, S. A. & Alexander, P. Macrophage content of tumours in relation to metastatic spread and host immune reaction. *Nature* **250**, 667–669 (1974).
64. Heldin, C.-H., Rubin, K., Pietras, K. & Ostman, A. High interstitial fluid pressure — an obstacle in cancer therapy. *Nat. Rev. Cancer* **4**, 806–813 (2004).
65. Swartz, M. A. & Lund, A. W. Lymphatic and interstitial flow in the tumour microenvironment: linking mechanobiology with immunity. *Nat. Rev. Cancer* **12**, 210–219 (2012).
66. Perrault, S. D., Walkey, C., Jennings, T., Fischer, H. C. & Chan, W. C. W. Mediating tumor targeting efficiency of nanoparticles through design. *Nano Lett.* **9**, 1909–1915 (2009).
67. Chauhan, V. P. *et al.* Fluorescent nanorods and nanospheres for real-time *in vivo* probing of nanoparticle shape-dependent tumor penetration. *Angew. Chem. Int. Ed. Engl.* **50**, 11417–11420 (2011).
68. Yuan, F. *et al.* Vascular permeability and microcirculation of gliomas and mammary carcinomas transplanted in rat and mouse cranial windows. *Cancer Res.* **54**, 4564–4568 (1994).
69. Albanese, A., Lam, A. K., Sykes, E. A., Rocheleau, J. V. & Chan, W. C. W. Tumour-on-a-chip provides an optical window into nanoparticle tissue transport. *Nat. Commun.* **4**, 2718 (2013).
70. Huang, X. *et al.* A reexamination of active and passive tumor targeting by using rod-shaped gold nanocrystals and covalently conjugated peptide ligands. *ACS Nano* **4**, 5887–5896 (2010).
71. Kunjachan, S. *et al.* Passive versus active tumor targeting using RGD- and NGR-modified polymeric nanomedicines. *Nano Lett.* **14**, 972–981 (2014).
72. Choi, C. H. J., Alabi, C. A., Webster, P. & Davis, M. E. Mechanism of active targeting in solid tumors with transferrin-containing gold nanoparticles. *Proc. Natl Acad. Sci. USA* **107**, 1235–1240 (2010).
73. Gordon, S. & Taylor, P. R. Monocyte and macrophage heterogeneity. *Nat. Rev. Immunol.* **5**, 953–964 (2005).
74. Fischer, H. C., Hauck, T. S., Gómez-Aristizábal, A. & Chan, W. C. W. Exploring primary liver macrophages for studying quantum dot interactions with biological systems. *Adv. Mater.* **22**, 2520–2524 (2010).
75. Huang, S. *et al. In vivo* splenic clearance correlates with *in vitro* deformability of red blood cells from *Plasmodium yoelii*-infected mice. *Infect. Immun.* **82**, 2532–2541 (2014).
76. Davies, L. C., Jenkins, S. J., Allen, J. E. & Taylor, P. R. Tissue-resident macrophages. *Nat. Immunol.* **14**, 986–995 (2013).
77. Syed, A. & Chan, W. C. W. How nanoparticles interact with cancer cells. *Cancer Treat. Res.* **166**, 227–244 (2015).
78. Patel, P. C. *et al.* Scavenger receptors mediate cellular uptake of polyvalent oligonucleotide-functionalized gold nanoparticles. *Bioconjugate Chem.* **21**, 2250–2256 (2010).
79. Wang, H., Wu, L. & Reinhard, B. M. Scavenger receptor mediated endocytosis of silver nanoparticles into J774A.1 macrophages is heterogeneous. *ACS Nano* **6**, 7122–7132 (2012).
80. Cedervall, T. *et al.* Understanding the nanoparticle–protein corona using methods to quantify exchange rates and affinities of proteins for nanoparticles. *Proc. Natl Acad. Sci. USA* **104**, 2050–2055 (2007).
81. Walkey, C. D. & Chan, W. C. W. Understanding and controlling the interaction of nanomaterials with proteins in a physiological environment. *Chem. Soc. Rev.* **41**, 2780–2799 (2012).
82. Albanese, A. *et al.* Secreted biomolecules alter the biological identity and cellular interactions of nanoparticles. *ACS Nano* **8**, 5515–5526 (2014).
83. Walkey, C. D., Olsen, J. B., Guo, H., Emili, A. & Chan, W. C. W. Nanoparticle size and surface chemistry determine serum protein adsorption and macrophage uptake. *J. Am. Chem. Soc.* **134**, 2139–2147 (2012).
84. Walkey, C. D. *et al.* Protein corona fingerprinting predicts the cellular interaction of gold and silver nanoparticles. *ACS Nano* **8**, 2439–2455 (2014).
85. Jong, W. H. de *et al.* Particle size-dependent organ distribution of gold nanoparticles after intravenous administration. *Biomaterials* **29**, 1912–1919 (2008).
86. Deen, W. M., Lazzara, M. J. & Myers, B. D. Structural determinants of glomerular permeability. *Am. J. Physiol. Renal Physiol.* **281**, F579–F596 (2001).
87. Venkatachalam, M. A. & Rennke, H. G. The structural and molecular basis of glomerular filtration. *Circ. Res.* **43**, 337–347 (1978).
88. Nair, A. V., Keliher, E. J., Core, A. B., Brown, D. & Weissleder, R. Characterizing the interactions of organic nanoparticles with renal epithelial cells *in vivo*. *ACS Nano* **9**, 3641–3653 (2015).
89. Pillai, G. Nanomedicines for cancer therapy: an update of FDA approved and those under various stages of development. *SOJ Pharm. Pharm. Sci.* **1**, 1–13 (2014).
90. Venditto, V. J. & Szoka, F. C. Cancer nanomedicines: so many papers and so few drugs! *Adv. Drug Deliv. Rev.* **65**, 80–88 (2013).
91. Allen, T. M. & Cullis, P. R. Liposomal drug delivery systems: from concept to clinical applications. *Adv. Drug Deliv. Rev.* **65**, 36–48 (2013).
92. Barenholz, Y. Doxil® — the first FDA-approved nano-drug: lessons learned. *J. Control. Release* **160**, 117–134 (2012).
93. Leonard, R. C. F., Williams, S., Tulpule, A., Levine, A. M. & Oliveros, S. Improving the therapeutic index of anthracycline chemotherapy: focus on liposomal doxorubicin (Myocet). *Breast* **18**, 218–224 (2009).
94. Chauhan, V. P. *et al.* Normalization of tumour blood vessels improves the delivery of nanomedicines in a size-dependent manner. *Nat. Nanotechnol.* **7**, 383–388 (2012).
95. Jiang, W., Huang, Y., An, Y. & Kim, B. Y. S. Remodeling tumor vasculature to enhance eelivery of intermediate-sized nanoparticles. *ACS Nano* **9**, 8689–8696 (2015).
96. Tailor, T. D. *et al.* Effect of pazopanib on tumor microenvironment and liposome delivery. *Mol. Cancer Ther.* **9**, 1798–1808 (2010).
97. Pastuskovas, C. V. *et al.* Effects of anti-VEGF on pharmacokinetics, biodistribution, and tumor penetration of trastuzumab in a preclinical breast cancer model. *Mol. Cancer Ther.* **11**, 752–762 (2012).
98. Dobosz, M., Ntziachristos, V., Scheuer, W. & Strobel, S. Multispectral fluorescence ultramicroscopy: three-dimensional visualization and automatic quantification of tumor morphology, drug penetration, and antiangiogenic treatment response. *Neoplasia* **16**, 1–13 (2014).
99. Roger, M. *et al.* Mesenchymal stem cells as cellular vehicles for delivery of nanoparticles to brain tumors. *Biomaterials* **31**, 8393–8401 (2010).
100. Li, L. *et al.* Silica nanorattle–doxorubicin-anchored mesenchymal stem cells for tumor-tropic therapy. *ACS Nano* **5**, 7462–7470 (2011).
101. Cheng, H. *et al.* Nanoparticulate cellular patches for cell-mediated tumoritropic delivery. *ACS Nano* **4**, 625–631 (2010).
102. Hu, Q. *et al.* Engineering nanoparticle-coated bacteria as oral DNA vaccines for cancer immunotherapy. *Nano Lett.* **15**, 2732–2739 (2015).
103. MacDiarmid, J. A. *et al.* Bacterially derived 400 nm particles for encapsulation and cancer cell targeting of chemotherapeutics. *Cancer Cell* **11**, 431–445 (2007).
104. Park, S. J. *et al.* New paradigm for tumor theranostic methodology using bacteria-based microrobot. *Sci. Rep.* **3**, 3394 (2013).
105. Doshi, N. *et al.* Cell-based drug delivery devices using phagocytosis-resistant backpacks. *Adv. Mater.* **23**, H105–H109 (2011).
106. Akin, D. *et al.* Bacteria-mediated delivery of nanoparticles and cargo into cells. *Nat. Nanotechnol* **2**, 441–449 (2007).
107. Kuhn, S. J., Finch, S. K., Hallahan, D. E. & Giorgio, T. D. Proteolytic surface functionalization enhances *in vitro* magnetic nanoparticle mobility through extracellular matrix. *Nano Lett.* **6**, 306–312 (2006).
108. Cui, M. *et al.* Multifunctional albumin nanoparticles as combination drug carriers for intra-tumoral chemotherapy. *Adv. Healthcare Mater.* **2**, 1236–1245 (2013).
109. Gormley, A. J. *et al.* Plasmonic photothermal therapy increases the tumor mass penetration of HPMA copolymers. *J. Control Release* **166**, 130–138 (2013).
110. Diagaradjane, P. *et al.* Modulation of *in vivo* tumor radiation response via gold nanoshell-mediated vascular-focused hyperthermia: characterizing an integrated antihypoxic and localized vascular disrupting targeting strategy. *Nano Lett.* **8**, 1492–1500 (2008).
111. Ohara, Y. *et al.* Effective delivery of chemotherapeutic nanoparticles by depleting host Kupffer cells. *Int. J. Cancer* **131**, 2402–2410 (2012).
112. van Rooijen, N. & Sanders, A. Liposome mediated depletion of macrophages: mechanism of action, preparation of liposomes and applications. *J. Immunol. Methods* **174**, 83–93 (1994).
113. Diagaradjane, P., Deorukhkar, A., Gelovani, J. G., Maru, D. M. & Krishnan, S. Gadolinium chloride augments tumor-specific imaging of targeted quantum dots *in vivo*. *ACS Nano* **4**, 4131–4141 (2010).
114. Parodi, A. *et al.* Synthetic nanoparticles functionalized with biomimetic leukocyte membranes possess cell-like functions. *Nat. Nanotechnol.* **8**, 61–68 (2013).
115. Piao, J.-G. *et al.* Erythrocyte membrane is an alternative coating to polyethylene glycol for prolonging the circulation lifetime of gold nanocages for photothermal therapy. *ACS Nano* **8**, 10414–10425 (2014).
116. Rodriguez, P. L. *et al.* Minimal "self" peptides that inhibit phagocytic clearance and enhance delivery of nanoparticles. *Science* **339**, 971–975 (2013).
117. Barua, S. & Mitragotri, S. Challenges associated with penetration of nanoparticles across cell and tissue barriers: a review of current status and future prospects. *Nano Today* **9**, 223–243 (2014).
118. Pascal, J. *et al.* Mechanistic patient-specific predictive correlation of tumor drug response with microenvironment and perfusion measurements. *Proc. Natl Acad. Sci. USA* **110**, 14266–14271 (2013).
119. Koay, E. J. *et al.* Transport properties of pancreatic cancer describe gemcitabine delivery and response. *J. Clin. Invest.* **124**, 1525–1536 (2014).
120. Shao, K. *et al.* Nanoparticle-based immunotherapy for cancer. *ACS Nano* **9**, 16–30 (2015).
121. Zuckerman, J. E. *et al.* Correlating animal and human phase Ia/Ib clinical data with CALAA-01, a targeted, polymer-based nanoparticle containing siRNA. *Proc. Natl Acad. Sci. USA* **111**, 11449–11454 (2014).
122. Bangham, A. D., Standish, M. M. & Watkins, J. C. Diffusion of univalent ions across the lamellae of swollen phospholipids. *J. Mol. Biol.* **13**, 238–252 (1965).

Acknowledgements

The authors thank all authors of the studies that were surveyed for providing additional information on request to calculate the nanoparticle delivery efficiencies (Supplementary information S1 (table)).The authors thank M. Samarakoon and A. Göpferich for fruitful discussions. The authors also thank S. Patel, M. Chalsev, A. Mahmood, J. D. Mora, and Y. Y. Chen for creating the database system. W.C.W.C. acknowledges the Canadian Institutes of Health Research (CIHR), Natural Sciences and Engineering Research Council (NSERC), and Prostate Cancer Canada for supporting his research program. H.F.D. acknowledges financial support from the US National Institutes of Health (NIH) grant P01 CA92644 and by a contract from the National Foundation for Cancer Research. S.O. acknowledges the Japan Society for the Promotion of Science (JSPS) for a Research Fellowship (PD, No. 5621) and the Ministry of Education, Culture, Sports, Science and Technology (MEXT) of Japan for a Grant-in-Aid for Young Scientists (B) (No. 26820356).

Competing interests statement

The authors declare no competing interests.

DATABASE

Cancer Nanomedicine Repository (CNR): http://inbs.med.utoronto.ca/cnr/ (June 2016)

SUPPLEMENTARY INFORMATION

See online article: S1–S8